Gravity Wave Spectra from GPS/MET Occultation Observations

A. K. STEINER AND G. KIRCHENGAST

Institute for Meteorology and Geophysics, University of Graz, Graz, Austria

(Manuscript received 9 September 1998, in final form 7 June 1999)

ABSTRACT

The potential utility of radio occultation data in general, and of data from the Global Positioning System/Meteorology (GPS/MET) experiment in particular, for studying atmospheric gravity waves is discussed. Based on a validated set of ~270 GPS/MET-derived temperature profiles, the authors produced and analyzed mean vertical wavenumber power spectra of normalized temperature fluctuations in three latitude bands (low, middle, high) within the lower stratosphere (~15–30 km), where data accuracy was proven highest. The Fresnel diffraction limited vertical resolution and the limited height range of the dataset restricted this initial investigation to medium- to large-scale waves with vertical wavelengths of about 2–5 km. The deduced vertical wavenumber power spectra were compared with a saturation spectrum predicted by gravity wave saturation theory and generally found consistent with the theoretical saturation limit. The low-latitude power spectra exhibited almost saturation, with spectral power about twice as high than at mid- to high latitudes. Dominant fluctuations were observed to occur at wavelengths of about 3–5 km, indicating the wave structures to be interpreted either as inertio–gravity waves or Rossby–gravity waves. A tendency was found, though, of increasingly underestimating spectral power toward shorter wavelengths. This very likely roots in weaknesses of the ''standard'' GPS/MET temperature retrieval applied here, which involves a geometrical optics, a local spherical symmetry, and a hydrostatic equilibrium assumption, all of which are increasingly violated toward smaller-scale wave structures and lead to an (artificial) wave smoothing in the retrieved temperature profiles. More elaborated future wave analyses should therefore employ improved retrieval methodology alleviating these assumptions and the authors indicate clear directions to this end. Generally, the results demonstrate that radio occultation data indeed bear high potential not only for fields like weather and climate prediction and climate monitoring but also for the study of atmospheric wave activity and its important role in atmospheric momentum and energy budgets.

1. Introduction

The investigation of wave structures in the lower and middle atmosphere (surface to mesopause) has been conducted by the application of a wide variety of different observation techniques. Among these, especially radiosonde measurements, supplying wind velocity and temperature data, provided important information on wave climatology, sources, and effects in the lower atmosphere (Allen and Vincent 1995; Vincent et al. 1997). Further techniques provided important results, including rocketsonde measurements (e.g., Dewan et al. 1984), balloon soundings (e.g., Fritts et al. 1988; Nastrom et al. 1997), radar observations (e.g., Fritts et al. 1990; Murayama et al. 1992; Vincent et al. 1997), and lidar studies (e.g., Wilson et al. 1991). Since all these (ground-based) observations are primarily confined to land-based sites in more industrialized regions, their spatial distribution shows a disadvantageous concentration over specific parts of Northern Hemisphere landmasses. This raises the problem of insufficient data for establishing wave climatologies on a global scale, despite the good temporal and spatial resolution of profiles from many of the ground-based instruments.

The advantages of spaceborne radio occultation observations of earth's atmosphere in general, and of the Global Positioning System/Meteorology (GPS/MET) measurements in particular, are that this technique can furnish atmospheric profiles with global coverage as well above oceans as above land, with high vertical resolution (<1 km) and accuracy (e.g., temperature <1 K within the upper troposphere and lower stratosphere), and under all weather conditions due to virtual insensitivity to clouds (see, e.g., the recent comprehensive study by Kursinski et al. (1997), for detailed information on the technique). The sensitivity of radio occultation observations to vertical wave structures was demonstrated by analyses of nonterrestrial planetary radio occultation data acquired during interplanetary spacecraft flybys at Titan, Jupiter, Uranus, Neptune, and Venus (Hinson and Tyler 1983; Allison 1990; Hinson and Magalhães 1991, 1993; Hinson and Jenkins 1995). There, retrieved temperature profiles as well as scintillations in

Corresponding author address: Andrea K. Steiner, Institute for Meteorology and Geophysics, University of Graz, Halbaerthgasse 1, A-8010 Graz, Austria.
E-mail: andi.steiner@kfunigraz.ac.at

occulted signal intensity were analyzed for the interpretation of gravity waves.

Initial qualitative discussions of wave structures seen in individual temperature profiles retrieved from the GPS/MET experiment, the first GPS-based occultation sounding of earth's atmosphere, were given by Kursinski et al. (1996, 1997) and Hocke (1997). Belloul and Hauchecorne (1997) recently investigated, based on simplified but reasonable simulations, how accurate occultation data can resolve gravity waves when using ''standard'' retrieval methodology. They concluded that a quantitative global study of wave activity should be well possible.

This study provides such a first investigation of the potential of terrestrial occultation data, here from the GPS/MET experiment, for global observation and analysis of gravity wave activity and is organized as follows. Section 2 briefly introduces into the key roles of gravity waves in the lower and middle atmosphere, their sources, morphology, and power spectra characteristics. Section 3 describes the GPS/MET observations, our temperature retrieval and validation procedure, and especially the gravity wave analysis based on the GPS/MET temperature profiles. The calculated power spectra of normalized temperature fluctuations are then discussed and interpreted in section 4. Section 5 gives our summary and conclusions.

2. Atmospheric gravity waves

The important role of internal gravity waves (GWs) in the atmosphere was first recognized by Hines (1960). Gravity waves are a major mechanism for transporting momentum and energy upward through the atmosphere and account for a significant portion of the spectrum of atmospheric motions and also importantly contribute to shape the thermal structure of the lower and middle atmosphere (e.g., Gossard and Hooke 1975; Lindzen 1990). In the middle atmosphere, they generate shear or dynamical instabilities and act to decelerate the mean flow in the mesosphere (e.g., Lindzen 1981). In turn, they themselves respond sensitively to wind shear and changes in the background stratification so that observations of propagating waves can help reveal characteristics of the basic atmospheric structure and circulation. Two important fundamental properties of GWs are their downward phase front progression despite their upward energy propagation (due to a dispersion relation projecting hyperbolic isofrequency curves on the horizontal-versus-vertical wavenumber plane) and their tendency to grow in amplitude with height proportional to the inverse square root of the, exponentially decreasing, air density (due to the law of conservation of energy).

a. Gravity wave sources and morphology

Disregarding upper atmospheric GWs of high interest in other contexts (e.g., Kirchengast 1996; Hocke and Schlegel 1996), GWs are mainly generated in the troposphere. Shear instabilities in the planetary boundary layer are suggested to generate short-scale GWs with wavelengths of a few kilometers and periods near 10 minutes (Nagpal 1979). Medium-scale GWs, with typical horizontal wavelengths of order 100 to 1000 km, vertical wavelengths of order 1 to 10 km, and periods of order 10 min to 1 h, are mainly excited due to phenomena such as the unstable behavior of jet streams, various meteorological disturbances such as fronts, thunderstorms and cumulonimbus convection, or penetrative convection in the lower troposphere and wind flows over irregular topography.

At equatorial latitudes, tropospheric heat sources (latent heat release) related to cumulus convection organized by synoptic-scale disturbances generate large-scale waves with zonal wavelengths of about 10 000 km, vertical wavelengths of near 5 km, and periods in the range of 4 to 5 days, which are known as mixed Rossby–gravity waves. Another type of long-period, vertically propagating waves in the lower stratosphere with zonal wavelengths spanning the full circumference of the earth (~40 000 km), vertical wavelengths of near 10 km, and periods in the 12- to 20-day range are planetary Kelvin waves (e.g., Holton 1972). These equatorial waves couple tropospheric convective activity to stratospheric circulation. In particular, the theory of the quasibiennial oscillation couples Kelvin and Rossby–gravity waves to the zonal wind pattern of the lower stratosphere (e.g., Andrews et al. 1987; Lindzen 1990).

b. Gravity wave power spectra characteristics

A key finding of many experimental studies on wavenumber and frequency power spectra of atmospheric GW motions was that their spectral characteristics are widely uniform in frequency and wavenumber, despite different generation sources, meteorological conditions, and locations of observations. Based on these studies and similar ones of oceanic gravity wave power spectra, VanZandt (1982) introduced the concept of a ''universal'' spectrum of atmospheric GWs, which much eases the task of developing globally useful but still efficient parameterization schemes of the influence of GWs on the mean atmospheric state (e.g., Fritts and VanZandt 1993; Hines 1997). A fact important for this study is that the power spectral density (PSD) of vertical wavenumber spectra does not follow the general rule of GW amplitude growth with height noted early in this section, but is almost constant with altitude throughout the middle atmosphere, especially at larger wavenumbers (e.g., Smith et al. 1987). This points to dissipative processes and saturation, for restoring total energy conservation validity, and several theories were developed to explain the physical mechanism responsible for limiting the wave amplitude growth (e.g., Dewan and Good 1986; Smith et al. 1987).

For our aim of obtaining a convenient vertical wave-

number PSD saturation limit for interpreting temperature fluctuations, we follow the saturation theory put forth by Smith et al. (1987) in the form applied by Allen and Vincent (1995) to temperature fluctuations [the original application by Smith et al. (1987) was to wind velocity fluctuations]. The respective formula for the PSD saturation limit of normalized temperature fluctuations reads, as a function of wavenumber (inverse vertical wavelength),

$$E_T(1/\lambda_Z) \approx \frac{\omega_B^4}{6g^2}\frac{1}{p}\frac{1}{(2\pi)^2}\frac{1}{(1/\lambda)^3}. \qquad (2.1)$$

In Eq. (2.1), λ_Z denotes the vertical wavelength, ω_B the Brunt–Väisälä frequency (see section 3b), g (=9.81 m s^{-2}) the acceleration of gravity, and p the slope of the GW's one-dimensional intrinsic frequency spectrum, which we set to $p = 5/3$ following common practice (see, e.g., Vincent et al. 1997). Equation (2.1) represents Eq. (8) of Allen and Vincent (1995) and the reader is referred for details on its derivation and its relation to the work of Smith et al. (1987) to that paper.

We will use the saturation limit expression, Eq. (2.1), below in the discussion of our GW analysis based on GPS/MET temperature retrievals. As to the reasonableness of using temperature profiles for creating GW spectra, Allen and Vincent (1995) showed that vertical wavenumber spectra of normalized temperature fluctuations are well suited to represent vertical wavenumber spectra of GWs.

3. GPS/MET data processing and gravity wave analysis

The successful installation of the navigation satellites of the U.S. GPS and the Russian GLONASS system, and the precise determination of satellite positions and velocities feasible in the meantime, recently opened up the attractive possibility for routinely probing the global terrestrial atmosphere by the radio occultation method. A first test of this concept was the GPS/MET ''proof-of-concept'' experiment, led by the University Corporation for Atmospheric Research (UCAR; Ware et al. 1996). According to the characteristic geometry of such GPS/GLONASS-based occultation sounding, the high-performance, dual-frequency GPS/MET navigation signal receiver aboard the small research satellite MicroLab1 performed active limb sounding based on GPS-to-MicroLab1 radio links. After its launch in April 1995 into a near-circular Low Earth Orbit (LEO), the GPS/MET receiver provided typically more than a hundred occultation events per scheduled observation day. The mission, collecting data until mid 1997, was the first successful phase of plans to develop a worldwide constellation of LEO satellites, which shall operationally provide a dense globally distributed dataset of fundamental atmospheric variables.

Each GPS satellite continuously transmits signals at two L-band carrier frequencies, 1575.42 MHz (L1) and 1227.6 MHz (L2), corresponding to wavelengths of ~19.0 cm (L1) and ~24.4 cm (L2), respectively. The GPS/MET receiver, by tracking these signals while occulted by the atmosphere, provided accurate measurements of excess phase and signal amplitude variation caused by the refractive properties of the atmosphere, which in turn depend on fundamental variables like temperature and humidity. Data of best quality, termed ''prime-time'' data (Rocken et al. 1997), were obtained when the encryption of the GPS signals (antispoofing) was turned off, and both L1 and L2 data were sampled at 50-Hz rate with equal performance. A subset of such ''prime-time'' measurements has been the basic dataset of this study.

a. Retrieval and validation of temperature profiles

The temperature profiles analyzed here with respect to waves were derived following the retrieval procedure described in detail by Steiner et al. (1999). Briefly, this procedure contains the usual three-step processing chain from excess phase measurements via atmospheric bending angles to refractivity, from which finally density, pressure, and temperature are deduced. Fundamentally involved is the geometric optics assumption (e.g., Born and Wolf 1980), which implies a vertical resolution limit of the temperature profiles of about 1–1.5 km in the stratosphere (Melbourne et al. 1994). In the first step from phases to atmospheric bending angles a heuristic statistical optimization scheme is involved (Hocke 1997; Hocke et al. 1997), which effectively prevents errors at mesospheric heights (to which the method is most susceptible) from degrading accuracy in our height range of interest below 35 km. The retrieval of refractivity profiles from bending angles was performed by a matrix inversion technique employing the commonly used Abel transform, which involves the assumption of local spherical symmetry about the profile location. Density, pressure, and temperature profiles were then deduced from refractivity employing the equation of state and the assumption of local hydrostatic equilibrium in a dry atmosphere (water vapor effects are negligible in our height range of interest above 10 km). The horizontal resolution related to such occultation profiles, somewhat depending on definition, is ~300 km (Melbourne et al. 1994; Kursinski et al. 1997) in the stratosphere.

We validated the full temperature dataset used here by comparison to colocated profiles from atmospheric analyses of the European Centre for Medium-Range Weather Forecasts (ECMWF). The validation results have been described in detail by Steiner et al. (1999), as well. They demonstrated, in line with other recent independent validation studies (Kursinski et al. 1996; Rocken et al. 1997), the accuracy of GPS/MET-derived temperature profiles to be very likely better than 1 K in the lower stratosphere (mean bias against good-quality ECMWF data <0.5 K, rms deviation <1.5 K).

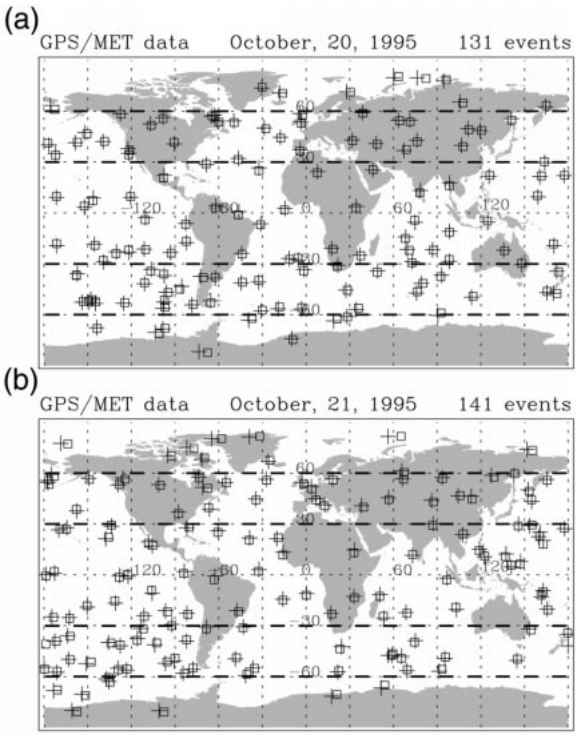

FIG. 1. Distribution and number of occultation events for 20–21 Oct 1995 used for the gravity wave analysis of GPS/MET data. Heavily dashed latitude circles delimit the three selected latitudinal bands: low latitudes (30°S to 30°N), middle latitudes (30° to 60°N/S), and high latitudes (60° to 90°N/S). Each individual event location is spotted by the tangent point of a high-altitude (mesospheric) occultation ray (center of square symbol) and of the bottommost (tropospheric) ray (plus symbol). The tangent point data were taken from the ''occultation tables'' at the UCAR GPS/MET data server.

b. Gravity wave analysis using GPS/MET temperature profiles

We used our validated temperature data set derived from GPS/MET data of 20 and 21 October 1995, a 2-day subset of ''prime-time 3'' data (Steiner et al. 1999). The whole data sample consists of 272 occultation events, the total number of events available for these two days of observations. We divided the data set into three subsets representing profiles at low (30°S to 30°N, 102 events), middle (30°N/S to 60°N/S, 136 events), and high (60°N/S to 90°N/S, 34 events) latitudes. Figure 1 illustrates the distribution and number of occultation events. The height sampling of the original profiles is unequal, ranging from ~200 m in the upper stratosphere to ~50 m in the troposphere. For providing equidistant height steps required for the spectral analysis, we interpolated the data to a regular 200-m grid.

We restricted the height range of the wave analysis to ~15 to 30 km, where GPS/MET data accuracy was proven highest (basic range ~10 to 35 km, but several kms need be dismissed near the edges due to filtering, see below). Above 35 km the accuracy is presumably degraded, since the retrieval procedure is increasingly susceptible to residual errors. Below 10 km the situation is encountered that GPS/MET raw profiles often stop between 5 and 10 km, degrading the database, and below ~8 km also water vapor effects need additional care.

A next step was to separate, in the temperature profiles, the background from the wave activity. This needs caution, since there exists in fact no sharp natural boundary between background and large wavelength waves and since also the background profile can contain small-scale structure, the most notable feature being the sharp equatorial tropopause. We found as most reasonable separation method, suitable for the full height range, to apply a Cos^2-filter with a cutoff wavenumber of 1/(8 km). We thus chose this filtering, which provided a better representation of background profiles than, for example, fitting a low-order polynomial as done by Vincent et al. (1997). The filter formally restricts our analysis to waves with vertical wavelengths <8 km, which is not seriously relevant, however, given the total height range of ~15 km.

Figure 2 depicts two representative temperature profiles, retrieved from GPS/MET data by the processing outlined in section 3a, which indicate wave activity. Figure 2a shows, to give one example, a profile spanning the full troposphere–stratosphere height range. While one can have good confidence in the wave structures <35 km, the upper stratospheric wave structures seen in this profile, and frequently in results of other processing chains similar to ours, are presumably spurious and a manifestation of measurement errors imperfectly treated by such retrieval procedures not optimized for higher altitudes. The lower panel concentrates on our height range of interest and illustrates the described filtering by comparing an original profile to its background profile obtained by the filtering agreement.

Based on original profile (T) and background profile ($\overline{T}$), we computed the normalized temperature fluctuation profile ($\hat{T}'$) by the usual expression,

$$\hat{T}' = \frac{T - \overline{T}}{\overline{T}}. \tag{3.1}$$

The $\hat{T}'$ profiles were then transformed to wavenumber space by applying a Fast Fourier Transform (FFT) algorithm with zero padding and computing the PSD as a function of vertical wavenumber (cycles km^{-1}). Finally, an average vertical wavenumber power spectrum was calculated for each of the three selected latitudinal bands. For comparison of the average vertical wavenumber power spectra with the saturation limit given by Eq. (2.1), we computed the Brunt–Väisälä frequency, ω_B, by evaluating

$$\omega_b^2 = \frac{(\gamma - 1)}{\gamma} \frac{g^2}{R_d T} + \frac{g}{T} \frac{dT}{dz}, \tag{3.2}$$

where γ (=1.4) and R_d (=287 J K^{-1} kg^{-1}) denote the ratio of specific heats and the gas constant for dry air, respectively. The second term of Eq. (3.2) naturally van-

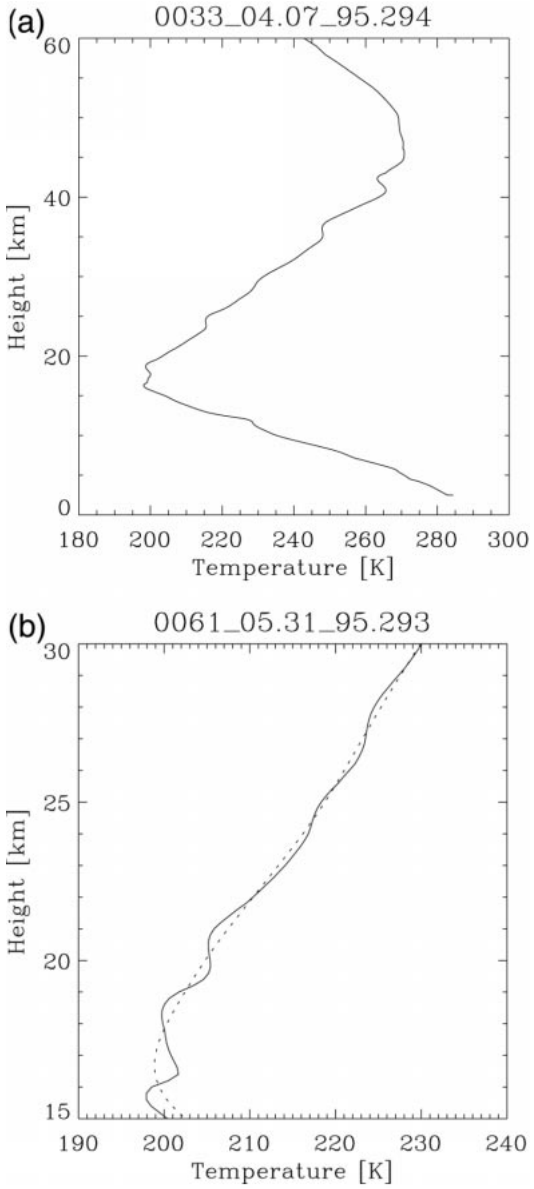

FIG. 2. Representative temperature profiles retrieved from GPS/MET data. (a) Full-height range example profile retrieved from occ.event 33, 0406 UTC 21 Oct 1995, located at 1.6°S and 51.2°W. (b) an original (solid) and its background (dotted) profile within the height range 15–30 km used for gravity wave analysis. The original profile was retrieved from occ.event 61, 0732 UTC 20 Oct 1995, located at 3.1°N and 34.8°E.

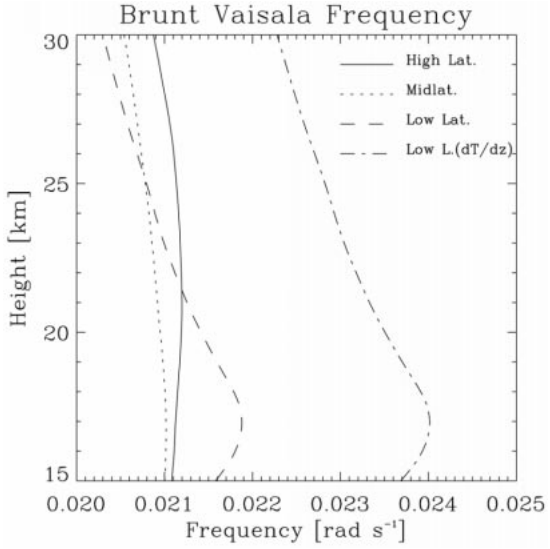

FIG. 3. Brunt–Väisälä frequency computed from the mean temperature profiles at low (dashed line), middle (dotted line), and high (solid line) latitudes, ignoring the temperature-gradient term in Eq. (3.2). For comparison, the Brunt–Väisälä frequency for equatorial latitudes is also shown with inclusion of the temperature-gradient term in Eq. (3.2) (dashed–dotted line).

ishes in an isothermal atmosphere but should also be small for the real atmosphere. In order to ensure a good estimate of ω_B, we computed its profile for each latitude band based on the corresponding mean temperature profile. Figure 3 shows plots of ω_B profiles for the three bands and confirms that it is weakly sensitive to actual thermal structure and well represented by a constant for the global lower stratosphere. Nonisothermality did not exert much influence on the magnitude of ω_B even in the low latitude region. For the calculation of the saturation limit we thus took a reasonable constant value of $\omega_B = 0.021$ rad s^{-1}, corresponding to a Brunt–Väisälä period of ~5 min, typical for the lower stratosphere.

4. Wavenumber spectra results and discussion

Figure 4 presents the vertical wavenumber power spectra obtained by our analysis for the low-, middle-, and high-latitude bands, respectively. For comparison purposes, the saturation limit obtained by Eq. (2.1) is indicated in each panel (heavy line). The spectral region of main interest corresponds to 2 to 5 km wavelengths (''main interval'' hereafter), where we expect best accuracy, but for convenience of discussion we show a broader interval spanning a range of wavelengths from 1 to 10 km, at the outer parts of which we certainly cannot expect our present analysis to produce reliable PSD. For indicating the sensitivity of each spectrum to the absolute choice of the 15-km analysis interval, we show not only the baseline case for the 15–30-km interval but three additional cases with the interval shifted in 1-km steps, up to 18–33 km. The sensitivity is reasonably weak—as should be—in the main interval, but there is nevertheless evidence that the background filtering should be further improved in future more elaborated studies, especially in clearing (or possibly even excluding) sharp tropopause features (cf. Allen and Vincent 1995).

The plots reveal that the PSD is roughly twice as high at low latitudes than at mid and high latitudes (comparing the 18–33-km interval, where the low latitude

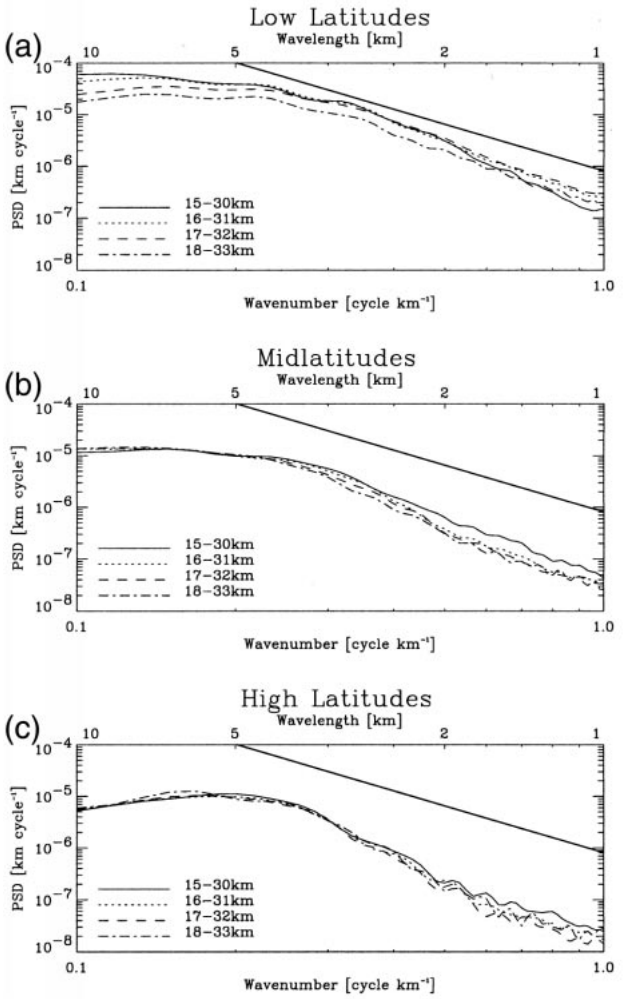

FIG. 4. Vertical wavenumber power spectra of normalized temperature fluctuations within the analyzed lower stratosphere height range. Double logarithmic plots show the power spectra for (a) low, (b) middle, and (c) high latitudes. A saturation spectrum (heavy solid line) is shown for reference. Four alternative analysis height ranges, 15–30 (solid), 16–31 (dotted), 17–32 (dashed), and 18–33 km (dashed–dotted lines), have been used.

spectrum is least influenced by residual background tropopause). This finding is in good agreement with the results of Allen and Vincent (1995), who analyzed temperature data from radiosonde measurements covering a latitude range of 12°–68°S. They found a significant latitudinal gradient in wave activity with the highest levels of activity in the Tropics. The results agree also reasonably well with stratospheric wave spectra of normalized temperature from balloon soundings at midlatitudes presented by Nastrom et al. (1997).

At low wavenumbers less than 0.2 cycles km^{-1}, corresponding to vertical wavelengths >5 km, the power spectra show a flattening, which is mostly due to the filter cutoff near 8 km. The PSD in this interval should therefore not be quantitatively interpreted in terms of GW spectra. In a more elaborated study, it will be worthwhile to extend the analyzed height range significantly beyond 15 km, which will then allow to estimate reasonable PSDs also for wavelengths >5 km.

At high wavenumbers greater than 0.5 cycles km^{-1} corresponding to vertical wavelengths <2 km, the PSD exhibits a damped slope toward less saturation, while there is convincing evidence from other studies that it should saturate (e.g., Allen and Vincent 1995; Nastrom et al. 1997). This tendency to underestimate saturation already gradually starts in the main interval, especially at middle and high latitudes. The very likely cause of this underestimation are weaknesses in the ''standard'' temperature retrieval methodology here applied, which involves (see section 3a) a geometric optics, a local spherical symmetry, and a hydrostatic equilibrium assumption in the processing. All of these are increasingly unrealistic towards smaller-scale wave structures and lead to increasingly suppressed wave amplitudes in the retrieved temperature profiles and, in turn, to PSDs increasingly underestimated at higher wavenumbers. More elaborated future wave studies should therefore alleviate these assumption by improved retrieval methodology. Though such alleviation efforts have been beyond the scope of this initial study, ways exist which we shall briefly outline below and which have already been demonstrated in other contexts.

The geometric optics assumption (leading to the Fresnel-limited vertical resolution of about 1–1.5 km in the stratosphere; see section 3a) can be overcome by employing diffraction–deconvolution techniques demonstrated to allow achievement of vertical resolutions near 100 m (e.g., Karayel and Hinson 1997).

The assumption of local spherical symmetry needs auxiliary (experimental or model) information to be rigorously overcome, but it was shown by Belloul and Hauchecorn (1997) that it, favorably, leads to appreciable damping of wave structures only at wavelengths shorter than the mean horizontal resolution (300 km; see section 3a) of occultation profiles. Thus not only large-scale but also a major range of medium-scale waves can be studied based on occultation data, even with spherical symmetry assumed. Further significant improvement of high-wavenumber parts of average GW spectra involving this assumption can be expected from a PSD correction based on a statistical quantification of the effects of spherical symmetry on medium- to short-scale waves, which should be well possible by quasi-realistic simulations or empirical modeling (asymptotically introducing saturation); somewhat similar to how radiosonde instrumental response was corrected for by Allen and Vincent (1995).

The hydrostatic assumption in retrieving pressure and temperature from density can be alleviated by suitably introducing the polarisation relation of gravity waves, which relates the amplitude and phase of pressure and temperature perturbations to the density perturbation. The latter, favorably, is known before any such assumption is introduced, since it is directly proportional

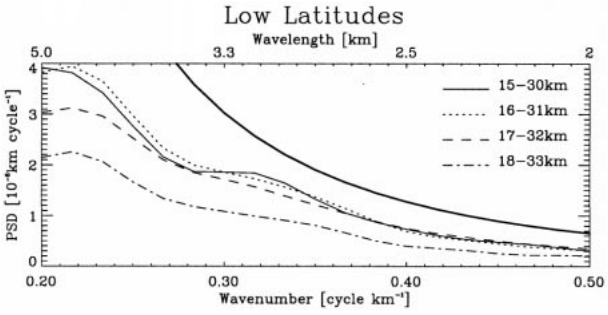

FIG. 5. Enlarged view of the main spectral interval of the low latitude power spectra of Fig. 4. The plot contents is identical to that of Fig. 4, top panel, but the PSD scale is now linear.

to refractivity (at the heights of interest above ~8 km, where water vapor effects are negligible). Alternatively, the utility of directly analyzing normalized density (or refractivity) fluctuations could be addressed, which completely avoids the hydrostatic assumption.

For the reasons above it is sensible to confine the interpretations of our present power spectra to the main interval between 0.2–0.5 cycles km^{-1}. Figure 5 zooms, now applying a linear PSD scale, into this main interval for the spectra of the low latitude band. On the one hand, it is much more visible now that the PSD of the 15–30-km spectrum is roughly twice as high than that of the 18–33-km spectrum, which very likely is due to the imperfectly removed sharp tropopause shape. On the other hand, it is highlighted that the PSD shape is fairly reasonable compared to other observational studies (e.g., Allen and Vincent 1995) in this main interval, which well demonstrates the utility of GPS occultation data for GW analysis.

Furthermore, Fig. 5 indicates spectral power to somewhat peak near 5 km and, weakly, also near 3 km in this low-latitude band, whereas at mid and high latitudes this indication is not found. Given the vertical wavelengths near 5 and 3 km one can identify these waves either as inertio–gravity or Rossby–gravity waves (e.g., Kursinski et al. 1996). Generally, the comparatively high power, or least tendency for PSD underestimation, in the low-latitude band also agrees with the fact that GW activity at medium to large scales, to which this initial analysis was well susceptible, is significantly more pronounced at lower than at higher latitudes. GPS occultation observations are thus particularly suited for characterizing equatorial waves. However, we believe that improved retrieval methodology as outlined above will allow to acquire reliable spectra over the full globe and for the major range of medium-scale GWs as well, within a height range of at least ~5 to 40 km.

5. Summary and conclusions

The aim of this study was to evaluate and discuss the potential and utility of GPS occultation data in general, and GPS/MET observations in particular, for the analysis of atmospheric gravity waves (GWs). After briefly introducing relevant characteristics of GWs and our methodology of retrieving and validating temperature profiles from GPS/MET occultation data, we described our analysis for producing vertical wavenumber spectra based on GPS/MET-derived normalized temperature fluctuations. Average spectra were computed within three latitude bands (low, middle, high) for the lower stratosphere. Due to Fresnel-diffraction limited vertical resolution (~1.5 km) and a limited analysis height range (~15–30 km), the reliable spectral interval (''main interval'') of this initial study is restricted to medium- to large-scale waves with vertical wavelengths of about 2 to 5 km. Emphasis was placed (section 4) on discussing and interpreting the result spectra complemented by a saturation spectrum estimate from GW saturation theory. Our main findings and conclusions are as follows.

1) The vertical wavenumber power spectra deduced from GPS/MET observations were found, in their main interval, to be generally consistent with the theoretical saturation limit proposed by Smith et al. (1987). The power spectra showed almost saturation in the low latitude band, with power spectral density roughly twice as high than at higher latitudes, in good agreement with results of Allen and Vincent (1995). Dominant fluctuations were observed to occur at wavelengths of near 3 and 5 km, indicating the wave structures to be interpreted either as inertio–gravity or Rossby–gravity waves.

2) A tendency of increasing underestimation of spectral power toward higher wavenumbers (vertical wavelengths <2 km) was noted, which already gradually started in the main interval, especially at middle and high latitudes. The very likely cause of this underestimation are weaknesses in the applied ''standard'' temperature retrieval methodology, which involves a geometric optics, a local spherical symmetry, and a hydrostatic equilibrium assumption. Since these assumptions are increasingly unrealistic toward smaller-scale wave structures, the wave amplitudes are increasingly suppressed by the retrieval technique and, consequently, the spectral power increasingly underestimated toward higher wavenumbers. More elaborated future studies should alleviate these assumptions and we have outlined ways to do so in the discussion section 4 above.

3) Despite the clearly stated limitations of this initial study, the results well demonstrate the utility of GPS/GLONASS occultation data for GW analysis. In particular, we showed this based on low latitude power spectra, which our ''standard'' retrieval methodology, most sensitive to medium- to large-scale waves, well captured within the main interval. We thus expect that improved retrieval methodology as outlined will allow to acquire reliable spectra over the full globe and for the major range of medium-scale GWs as well, down to subkilometer vertical wavelengths. Furthermore, improved occultation data quality due to improved future GPS/GLONASS receivers together with optimized re-

trievals will allow to at least double the analysis height range (e.g., allow 10–40 km), consequently, extending the spectral range for reliable power estimation at low wavenumbers to vertical wavelengths of ~10 km.

4) Allen and Vincent (1995) concluded that most variation of stratospheric GW activity occurs at low vertical wavenumbers (wavelengths >1 km), while the spectra at higher wavenumbers generally appear to be saturated (i.e., predictable by a saturation spectrum): Thus the occultation method could contribute global GW climatology just in the most needed wavenumber range corresponding to vertical wavelengths of ~1 to 10 km.

In summary, GPS/GLONASS radio occultation data indeed appear to be very valuable not only for applications like weather and climate modeling and prediction and climate change monitoring for which they are primarily collected, but also for the global study of atmospheric wave activity and its important role in atmospheric circulation and energy budgets.

Acknowledgments. We are grateful to GPS/MET Principal Investigator R. Ware, GPS/MET project managers M. Exner and C. Rocken, and the GPS/MET team at UCAR, Boulder, for operating the GPS/MET experiment and supplying the data. Furthermore, we thank H. P. Ladreiter, Inst. of Space Research/Austrian Academy of Sciences, Graz, for fruitful scientific discussions, and U. Foelsche, IMG/UoG, for cooperation in preparing Fig. 1.

The first author (A. K. Steiner) was financially supported for this work by IMG/UoG's ''ATFERN'' discretionary funds, by the K.&M. Kaufmann Foundation, Graz, Austria, and by the START-Programm No. Y103-CHE (START-ATCHANGE) research award of the Bundesministerium für Wissenschaft und Verkehr, Vienna, Austria.

REFERENCES

Allen, S. J., and R. A. Vincent, 1995: Gravity wave activity in the lower atmosphere: Seasonal and latitudinal variations. *J. Geophys. Res.,* **100,** 1327–1350.

Allison, M., 1990: Planetary waves in Jupiter's equatorial atmosphere. *Icarus,* **83,** 282–307.

Andrews, D. G., J. R. Holton, and C. B. Leovy, 1987: *Middle Atmosphere Dynamics.* International Geophysical Series, Vol. 40, Academic Press, 489 pp.

Belloul, M. B., and A. Hauchecorne, 1997: Effect of periodic horizontal gradients on the retrieval of atmospheric profiles from occultation measurements. *Radio Sci.,* **32,** 469–478.

Born, M., and E. Wolf, 1980: *Principles of Optics.* 6th ed. Pergamon Press, 808 pp.

Dewan, E. M., and R. E. Good, 1986: Saturation and the ''universal'' spectrum for vertical profiles of horizontal scalar winds in the atmosphere. *J. Geophys. Res.,* **91,** 2742–2748.

——, N. Grossbard, A. F. Quesada, and R. E. Good, 1984: Spectral analysis of 10-m resolution scalar velocity profiles in the stratosphere. *Geophys. Res. Lett.,* **11,** 80–83; Correction, **11,** 624.

Fritts, D. C., and T. E. VanZandt, 1993: Spectral estimates of gravity wave energy and momentum fluxes. Part I: Energy dissipation, acceleration, and constraints. *J. Atmos. Sci.,* **50,** 3685–3694.

——, T. Tsuda, T. E. VanZandt, S. A. Smith, T. Sato, S. Fukao, and S. Kato, 1990: Studies of velocity fluctuations in the lower atmosphere using the MU radar. Part II: Momentum fluxes and energy densities. *J. Atmos. Sci.,* **47,** 51–66.

——, ——, T. Sato, S. Fukao, and S. Kato, 1988: Observational evidence of a saturated gravity wave spectrum in the troposphere and lower stratosphere. *J. Atmos. Sci.,* **45,** 1741–1759.

Gossard, E. E., and W. H. Hooke, 1975: *Waves in the Atmosphere.* Developments in Atmospheric Science, Vol. 2, Elsevier Scientific Publishing Company, 456 pp.

Hines, C. O., 1960: Internal gravity waves at ionospheric heights. *Can. J. Phys.,* **38,** 1441–1481.

——, 1997: Doppler spread parameterization of gravity wave momentum deposition in the middle atmosphere. Part 2: Broad and quasi monochromatic spectra and implementation. *J. Atmos. Terr. Phys.,* **59,** 387–400.

Hinson, D. P., and G. L. Tyler, 1983: Internal gravity waves in Titan's atmosphere observed by Voyager radio occultation. *Icarus,* **54,** 337–352.

——, and J. A. Magalhães, 1991: Equatorial waves in the stratosphere of Uranus. *Icarus,* **94,** 64–91.

——, and ——, 1993: Inertio-gravity waves in the atmosphere of Neptune. *Icarus,* **105,** 142–161.

——, and J. M. Jenkins, 1995: Magellan radio occultation measurements of atmospheric waves on Venus. *Icarus,* **114,** 310–327.

Hocke, K., 1997: Inversion of GPS meteorology data. *Ann. Geophys.,* **15,** 443–450.

——, and K. Schlegel, 1996: A review of atmospheric gravity waves and travelling ionospheric disturbances: 1982–1995. *Ann. Geophys.,* **14,** 917–940.

——, G. Kirchengast, and A. K. Steiner, 1997: Ionospheric correction and inversion of GNSS occultation data: problems and solutions. IMG/UoG Tech. Rep. for ESA/ESTEC No.2/97, 35 pp. [Available from Inst. for Meteorology and Geophysics, University of Graz, Halbaerthgassel, A-8010 Graz, Austria.]

Holton, J. R., 1972: Waves in the equatorial stratosphere generated by tropospheric heat sources. *J. Atmos. Sci.,* **29,** 368–375.

Karayel, E. T., and D. P. Hinson, 1997: Sub-Fresnel-scale vertical resolution in atmospheric profiles from radio occultation. *Radio Sci.,* **32,** 411–423.

Kirchengast, G., 1996: Elucidation of the physics of the gravity wave—TID relationship with the aid of theoretical simulations. *J. Geophys. Res.,* **101,** 13 353–13 368.

Kursinski, E. R., and Coauthors, 1996: Initial results of radio occultation observations of Earth's atmosphere using the global positioning system. *Science,* **271,** 1107–1110.

——, G. A. Hajj, K. R. Hardy, J. T. Schofield, and R. Linfield, 1997: Observing Earth's atmosphere with radio occultation measurements using the Global Positioning System. *J. Geophys. Res.,* **102,** 23 429–23 465.

Lindzen, R. S., 1981: Turbulence and stress owing to gravity wave and tidal breakdown. *J. Geophys. Res.,* **86,** 9707–9714.

——, 1990: *Dynamics in Atmospheric Physics.* Cambridge University Press, 310 pp.

Melbourne, W. G., and Coauthors, 1994: The application of spaceborne GPS to atmospheric limb sounding and global change monitoring. JPL Publication 94-18, Jet Propulsion Lab, Pasadena, CA, 147 pp.

Murayama, Y., T. Tsuda, M. Yamamoto, T. Nakamura, T. Sato, S. Kato, and S. Fukao, 1992: Dominant vertical scales of gravity waves in the middle atmosphere observed with the MU radar and rocketsondes. *J. Atmos. Terr. Phys.,* **54,** 339–346.

Nagpal, O. P., 1979: The sources of atmospheric gravity waves. *Contemp. Phys.,* **20,** 593–609.

Nastrom, G. D., T. E. Van Zandt, and J. M. Warnock, 1997: Vertical wavenumber spectra of wind and temperature from high-resolution balloon soundings over Illinois. *J. Geophys. Res.,* **102,** 6685–6701.

Rocken, C., and Coauthors, 1997: Analysis and validation of GPS/MET data in the neutral atmosphere. *J. Geophys. Res.,* **102,** 29 849–29 866.

Smith, S. A., D. C. Fritts, and T. E. VanZandt, 1987: Evidence for a saturated spectrum of atmospheric gravity waves. *J. Atmos. Sci.*, **44,** 1404–1410.

Steiner, A. K., G. Kirchengast, and H. P. Ladreiter, 1999: Inversion, error analysis, and validation of GPS/MET occultation data. *Ann. Geophys.*, **17,** 122–138.

VanZandt, T. E., 1982: A universal spectrum of buoyancy waves in the atmosphere. *Geophys. Res. Lett.*, **9,** 575–578.

Vincent, R. A., S. J. Allen, and S. D. Eckermann, 1997: Gravity-wave parameters in the lower stratosphere. NATO ASI Series I, Global Environmental Change, Vol. 50, Springer-Verlag, 7–25.

Ware, R., and Coauthors, 1996: GPS Sounding of the atmosphere from Low Earth Orbit: Preliminary results. *Bull. Amer. Meteor. Soc.*, **77,** 19–40.

Wilson, R., M. L. Chanin, and A. Hauchecorne, 1991: Gravity waves in the middle atmosphere observed by Rayleigh lidar, 2. Climatology. *J. Geophys. Res.*, **96,** 5169–5183.